

BEHAVIOUR OF STEEL-TO-CONCRETE JOINTS II

Moment resisting joint of a composite beam to reinforced concrete wall

José Henriques ^a, Ana Ozbolt ^b, Jiří Žižka ^c, Ulrike Kuhlmann ^b, Luís Simões da Silva ^a and František Wald ^c

^a ISISE, Faculty of Sciences and Technology, University of Coimbra

^b Institute of Structural Design, University of Stuttgart

^c Department of Steel and Timber Structures, Czech Technical University in Prague

INTRODUCTION

Aiming at the study of steel-to-concrete joints, the RFCS project entitled “New market chances for steel structures by innovative fastening solutions” (“InFaSo” [1]) was launched. Within the experimental programme of the project, composite beam to reinforced concrete wall joints were tested. In the present paper, the results of these tests are presented. Subsequently, to determine joint properties a spring mechanical model has been developed and validated against the experimental results.

The studied joint configuration is illustrated in *Fig. 1*. Two different transfer areas may be distinguished. The upper area consists of a reinforced concrete slab where the longitudinal reinforcement is anchored in the reinforced concrete wall. The wall and the slab were concreted at different times and therefore, no shear is assumed to be transferred between these members. Any friction is neglected. Thus, only tension is transferred through this part of the joint. At the bottom area, the steel beam sits in a steel bracket welded to an anchor plate which is fastened the reinforced concrete wall. The fixation between anchor plate and wall is achieved by headed studs welded to the plate. On the outside of the steel bracket, a plate is welded creating a “nose” which avoids the slip of the beam out of the steel bracket. The end-plate of the steel beam is used for this propose. This end-plate transmits the shear load to the steel bracket. Finally, compression is transferred to the reinforced concrete wall using a contact plate between end-plate and anchor plate. The flux of loads is schematically represented in *Fig. 2* for a hogging bending moment.

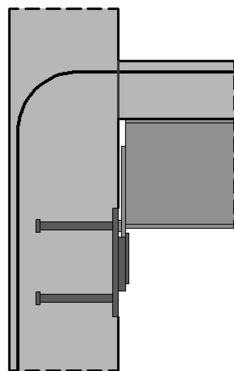


Fig. 1– Studied joint configuration

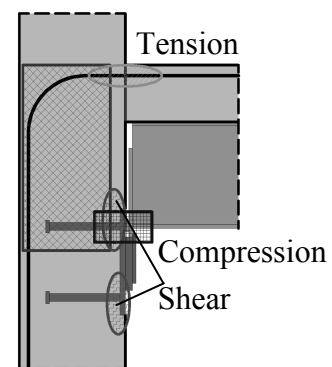


Fig. 2 - Flux of loads

1 EXPERIMENTAL RESEARCH

1.1 Description of the experimental programme

The test programme comprised a total of six tests. Three were performed at the University of Stuttgart (USTUTT) and the other three at the Czech Technical University in Prague (CTU). The reference test specimen configuration consists of a cantilever composite beam supported by a reinforced concrete wall (*Fig. 3*). The geometry of the test specimens was varied within each group of three tests. One specimen had the same geometric properties and therefore was common to both groups. Besides this common test specimens, the variation of geometry differed from one institution

to another. In Stuttgart, the variation consisted of the percentage of reinforcement in the slab and the disposition of the shear studs (a – distance of the first shear stud to the joint face) in the composite beam. In Prague, the geometric parameters thickness of the anchor plate and the steel bracket were varied. The varied geometric properties within the different test specimens are summarized in *Table 1*. The test procedure relied on applying a concentrated load at the free-end of the cantilever beam with a hydraulic jack up to failure. The tests were static monotonic. The reinforced concrete wall was fixed at bottom and top. In Fig. 4 the test layout is shown. The tests were performed using control of displacements. More detailed information about the tests may be found in [1].

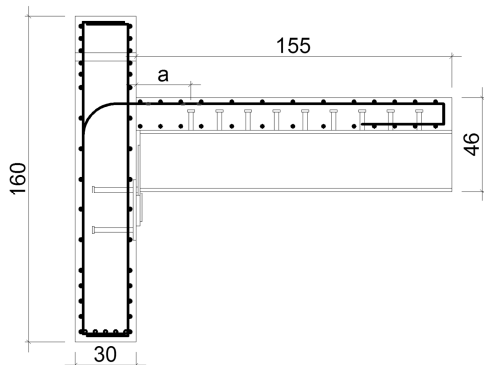


Fig. 3 – Test specimens' configuration(cm)

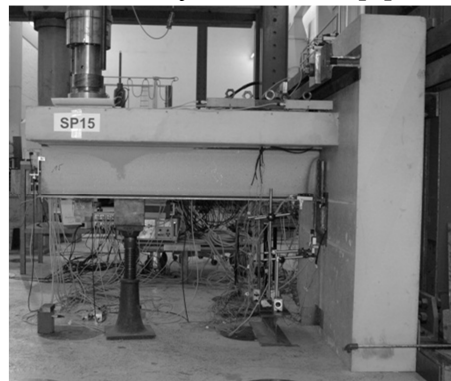


Fig. 4 – Test layout

Table 1 - Varied geometric properties of the test specimens.

Test ID	USTUTT			CTU in Prague		
	SP13	SP14	SP15	P15-20	P15-50	P10-50
$t_{\text{Anchor Plate}}$ [mm]	15	15	15	15	15	10
$t_{\text{Steel Bracket}}$ [mm]	20	20	20	20	50	50
$\Phi_{\text{slab reinf}}$ [mm]	16	12	16	16	16	16
a [mm]	500	270	270	270	300	300

1.2 Tests results

In all tests failure was attained by rupture of one of the longitudinal steel reinforcement bars in tension. This made the longitudinal steel reinforcement in tension the component governing the behaviour of the joint. The variations of the anchor plate and the steel bracket in the Prague tests did not produce any significant change of the mode of failure. In Fig. 5 and Fig. 6 the relative moment-rotation curves of all tested specimens are presented. A ductile failure is confirmed by the rotation capacity achieved in all tests.

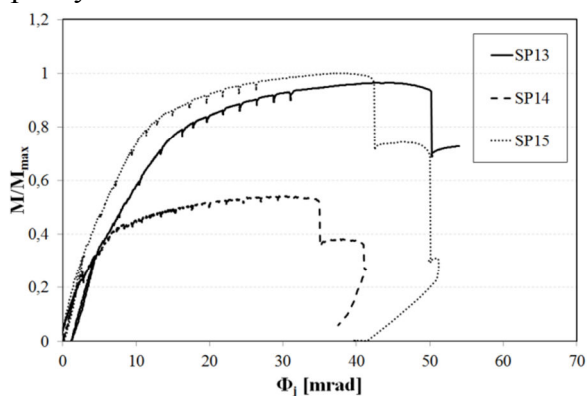


Fig. 5 – Relative moment-rotation curves obtained USTUTT tests

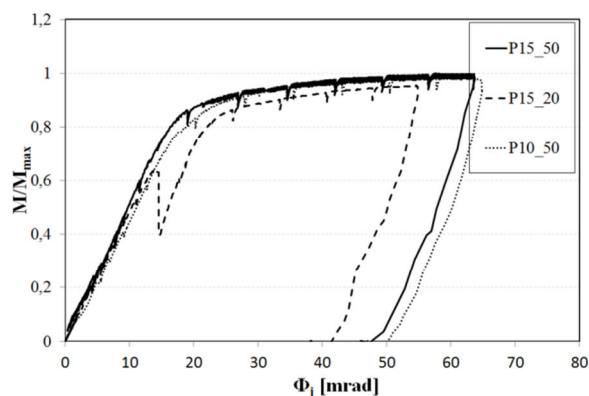


Fig. 6 – Relative moment-rotation curve obtained in CTU tests

1.3 Discussion of the test results

The Prague tests demonstrated that the variations of the anchor plate and steel bracket geometry did not affect significantly the results. As for the Stuttgart tests, the behaviour of the joint was completely governed by the longitudinal steel reinforcement. The variation of the percentage of reinforcement in the Stuttgart tests resulted in an obvious variation of the resistance; showing an increase between SP14 and the other tests SP13 and Sp15 of about 80%. In what concerns the effect of the position of the shear studs a , as observed in [2], there is an influence on the deformation capacity of the joint. The comparison between test specimen SP13 and SP15 reveals that higher ultimate rotation is obtained with higher value of a . This result is consistent with the experimental observations in [2]. For smaller values of a , the crack opening concentrates near the joint face resulting in a smaller elongation length contributing to the joint rotation. The slip in the shear connection of the composite beam was measured at 4 sections along the beam length. Higher slip was observed closer to the joint, and with the increase of the distance to the joint the slip diminished.

2 ANALYTICAL APPROACH

2.1 Joint model

Based on the joint configuration under study, the joint components listed in Table 2 are identified to contribute to the joint response. The joint components are numbered independently of the numbering provided by EN 1993-1.8 [3]. Accordingly, the spring mechanical model is built as illustrated in Fig. 7. In the model, three groups of springs are separated by two vertical rigid bars. The rigid bars allow avoiding the interplay between tension and compression components, simplifying the joint assembly. Another simplification is introduced by considering a single spring to represent the joint panel. The joint panel is the component representing the reinforced concrete wall in the region adjacent to the joint. For the behaviour of the reinforced concrete wall a much more sophisticated model has first to be derived in order to then “concentrate” its behaviour into this single spring. Concerning the tension springs, the slip and the elongation of the longitudinal reinforcement are assumed at the same level although in reality the slip is observed at the steel beam–concrete slab interface. Finally, regarding the group of compression components, components 5, 6 and 7, their concentration in a single spring results from simplifications performed after the detailed analysis of the anchor plate subjected to compression force. All the mentioned simplifications are justified and may be found in [1].

Table 2 - List of joint components

Nº	Basic joint component
1	Longitudinal steel reinforcement in tension
2	Slip of composite beam (due to incomplete interaction)
3	Beam web and flange in compression
4	Steel contact plate
5	Anchor plate in bending under compression
6	Concrete in compression
7	Anchor in tension
8	Joint panel

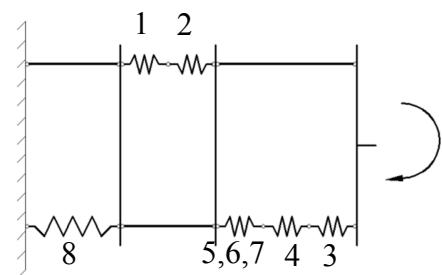


Fig. 7 – Joint component model

2.2 Components evaluation

As referred in 1.3, the longitudinal reinforcement in tension was the component governing the behaviour of the joint. Thus, the accuracy of the joint model will much depend on the sophistication introduced in the modelling of this component. A sophisticated model can be found in [4] where the

behaviour of longitudinal reinforcement is modelled taking into account the embedment in concrete, the component resistance is assumed up to the ultimate strength of the reinforcement. In this way, the component is modelled by means of a multi-linear force-displacement curve with hardening. The model assumes the resistance of the longitudinal steel reinforcement up to its ultimate resistance and allows estimating the corresponding deformation. This deformation is then assumed as the deformation capacity although in reality it should be higher. In EN 1994-1-1 [5] the component model is much simpler. It is assumed that the resistance is defined by the yielding capacity of the steel reinforcing bar and deformation is obtained by means of stiffness coefficients. Rotation capacity should be available if the longitudinal steel reinforcement in tension is the governing component. However, no guidance is provided to estimate the rotation capacity and the ductility is in dependence on the ductility class of the reinforcement. The two models, illustrated in *Fig. 8*, were applied and are compared with experimental tests.

The composite beam was designed to have full interaction between steel beam and RC slab; therefore, no limitation to the joint resistance was expected from component No. 2. In what concerns the deformation of this component, as verified in [6], a small contribution to the joint rotation may be observed. According to [7], the slip at the connection depends on the nearest stud to the wall face. Under increasing load this stud provides resistance to slip until it becomes plastic. Additional load is then assumed to be resisted by the next stud deforming elastically until its plastic resistance is reached. Further load is then carried by the next stud and so forth. The analytical model considered this approach. In the EN 1994-1-1 [5], the slip is taken into account by multiplying the stiffness coefficient of the longitudinal steel reinforcement in tension component by a slip factor. Again both models were applied. A complete description of the above components and of all components presented as listed in Table 2 is provided in [1]. However, it should be stated that the other components had a minor influence on the joint response and therefore some simplifications were considered.

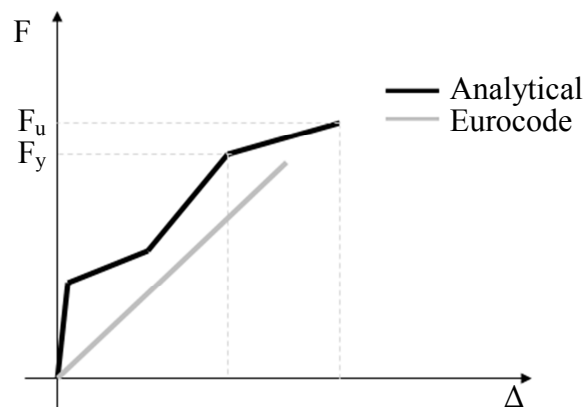


Fig. 8 – Behaviour of the longitudinal reinforcement component (1)

2.3 Model assembly

With the simplifications considered, as e.g. neglecting the joint panel component due to the wall dimensions and reinforcement detailing, and performing the assembly of the components per row, the joint model is simplified as illustrated in *Fig. 9*. Then, because only one tension row and one compression row are considered, the determination of the joint properties becomes relatively easy as expressed in equation (1) to (4). The application of the joint model and the comparison with experimental results is presented later in 3 for the analytical approach as well as following the code rules.

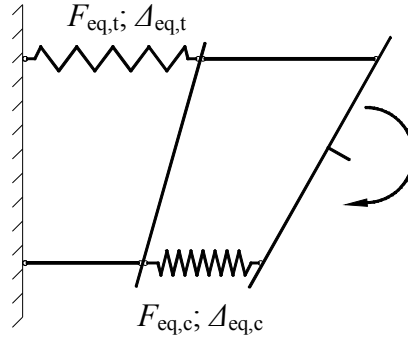


Fig. 9 – Simplified model after component rows assembly

$$F_{eq} = \text{Min}\{F_i \text{ to } F_n\} \quad (1)$$

$$\Delta_{eq} = \sum_{i=1}^n \Delta_i \quad (2)$$

$$M_j = \text{Min}\{F_{eq,t}; F_{eq,c}\}h_r \quad (3)$$

$$\phi_j = \frac{\Delta_{eq,t} + \Delta_{eq,c}}{h_r} \quad (4)$$

Where: F_i to F_n is the resistances of the individual components, separately for tension and compression; $F_{eq,t}$ and $F_{eq,c}$ are the resistance of the equivalent components, tension and compression, respectively; Δ_i is the deformation of the components; $\Delta_{eq,t}$ and $\Delta_{eq,c}$ are the deformations of the equivalent components, tension and compression, respectively; M_j and Φ_j is the joint bending moment and joint rotation, respectively; h_r is the lever arm of the joint.

3 APPLICATION OF THE JOINT MODEL AND COMPARISON OF RESULTS

The application of the joint model, considering the analytical and code approach, is presented and compared in *Fig. 10* and *Fig. 11*, by means of $M/M_{\max, \text{test}}-\Phi$ curves. Two test specimens with different load capacities were used: test specimen SP14 and SP15. The hardening considered in the code approach was determined assuming $S_{j, \text{ini}}$ up to $2/3M_j$ and the modification stiffness coefficient (ρ) was taken equal to 2, as for steel beam-to-column joints. In *Table 3* two ratios are presented, quantifying the approximation of the analytical and code models, for bending moment ($M_{\max, \text{model}}/M_{\max, \text{Test}}$) and rotation capacity ($\Phi_{u, \text{model}}/\Phi_{u, \text{Test}}$). In terms of resistance, both models present a very good approximation. Less accuracy is achieved for the rotation capacity however, given the difficulty to estimate this parameter also in tests, the approximation observed is promising. In the code so far, no provisions are given for the quantification of rotation capacity.

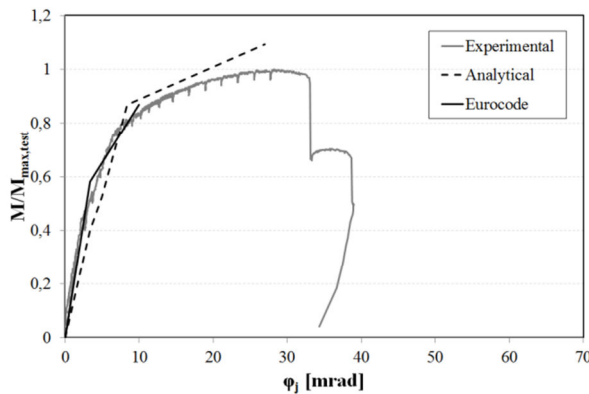


Fig. 10– M- Φ for test specimen SP14

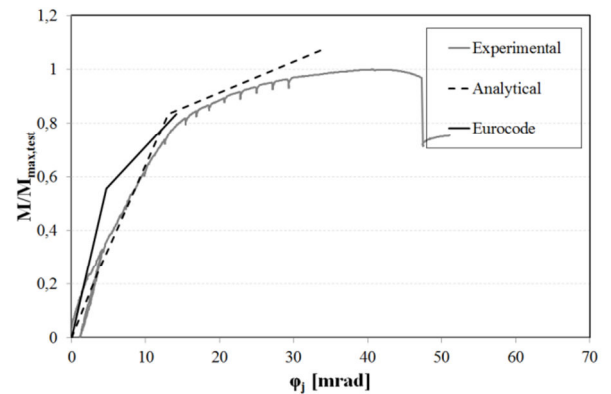


Fig. 11 – M- Φ for test specimen SP15

Table 3 – Comparison of results: ratio analytical model/test and Eurocode approach/test

Test ID	$M_{\max,An}/M_{\max,Test}$	$\Phi_{u,An}/\Phi_{u,Test}$	$M_{\max,EC}/M_{\max,Test}$	$\Phi_{u,EC}/\Phi_{u,Test}$
SP14	1,09	0,83	0,87	-
SP15	1,04	0,87	0,83	-

4 SUMMARY AND ACKNOWLEDGMENT

This paper has presented the research work on composite beam to reinforced concrete wall joints realized as part of a RFCS research project [1]. The solution investigated represents a joint configuration that, as it is one of the aims of this project, intends a simple and easy erection. The analytical model proposed reflected the simplicity of the joint solution. As the tests were governed by the longitudinal steel reinforcement in tension, more sophistication has been introduced in the model of this component. Two approaches were compared with test results which showed good accuracy; one based on the ECCS publication [4] where the behaviour of the longitudinal steel reinforcement takes into consideration the embedment in the concrete, and another based in EN 1994-1-1 [5]. The limited number of tests did not allow verifying other components like the joint panel or the slip at the interface of the steel beam and the concrete slab. This should further be analysed based on the numerical work under development.

The financial support from the European Commission by the Research Fund for Coal and Steel (RFCS) is gratefully acknowledged.

5 REFERENCES

- [1] Stuttgart University, “New market chances for steel structures by innovative fastening solutions”, Final report of the RFCS project N° RFS-PR-05062, 2011 (to be published).
- [2] Schäfer, M. “Zum Rotationsnachweis teiltragfähiger Verbundknoten in verschieblichen Verbundrahmen”, Doctoral Thesis, University of Stuttgart, July, 2005. (In German)
- [3] CEN, European Committee for Standardization, “Eurocode 3: Design of steel structures – Part 1-8: Design of joints”, EN 1993-1-8, Brussels, Belgium, May, 2005.
- [4] ECCS, “Design of Composite Joints for Buildings”, ECCS Publication n°109, Technical Committee 11, Composite Structures, First Edition, Belgium, 1999.
- [5] CEN, European Committee for Standardization, “Eurocode 4: Design of composite steel and concrete structures – Part 1-1: General rules and rules for buildings”, EN 1994-1-1, Brussels, Belgium, December, 2004.
- [6] Aribert, J. M. “Influence of Slip on Joint Behaviour”, Connections in Steel Structures III, Behaviour, Strength and Design, Third International Workshop, Trento, Italy, May 29-31, 1995.
- [7] Anderson, D.; Najafi, A. A. “Performance of Composite Connections: Major Axis End Plate Joints”, Journal of Constructional Steel Research, vol. 31, pp. 31-57, 1994.